

See discussions, stats, and author profiles for this publication at: <https://www.researchgate.net/publication/258078453>

Quenching of 5,5'-disulfopropyl-3,3'-dichlorothiacyanine Dye Adsorbed on Gold Nanoparticles

ARTICLE in THE JOURNAL OF PHYSICAL CHEMISTRY C · JANUARY 2013

Impact Factor: 4.77

CITATIONS

3

READS

72

7 AUTHORS, INCLUDING:



Vesna Vasić

Vinča Institute of Nuclear Sciences

95 PUBLICATIONS 917 CITATIONS

[SEE PROFILE](#)



Miroslav D Dramicanin

Vinča Institute of Nuclear Sciences

281 PUBLICATIONS 1,942 CITATIONS

[SEE PROFILE](#)



Sofija Sovilj

University of Belgrade

57 PUBLICATIONS 513 CITATIONS

[SEE PROFILE](#)



Vesna Vodnik

Vinča Institute of Nuclear Sciences

76 PUBLICATIONS 625 CITATIONS

[SEE PROFILE](#)

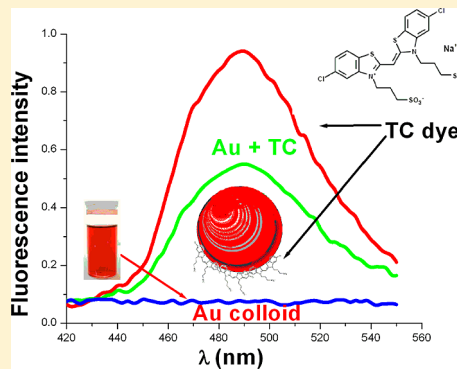
Fluorescence Quenching of 5,5'-Disulfopropyl-3,3'-dichlorothiacyanine Dye Adsorbed on Gold Nanoparticles

Ana Vujačić,[†] Vesna Vasić,[†] Miroslav Dramičanin,[†] Sofija P. Sovili,[‡] Nataša Bibić,[†] Slobodan Milonjić,[†] and Vesna Vodnik^{*,†}

[†]Vinča Institute of Nuclear Sciences, University of Belgrade, P.O. Box 522, 11158 Belgrade, Serbia

[‡]Faculty of Chemistry, University of Belgrade, P.O. Box 118, 11158 Belgrade, Serbia

ABSTRACT: Nanoparticles (NPs) modified with fluorescent cyanine dyes can exhibit fluorescent quenching properties due to energy and/or electron transfer, and these systems have many applications in catalysis, drug delivery, nanoelectronics, medical diagnostics, and chemical sensing. The aim of this work was to investigate the adsorption of cyanine dye 5,5'-disulfopropyl-3,3'-dichlorothiacyanine (TC) on the surface of citrate capped gold nanoparticles (AuNPs) with the average core sizes of 9, 17, and 30 nm using various experimental techniques. The measurements of fluorescence corrected for inner filter effects (IFE) of the particle–dye assembly clearly indicated that the fluorescence of TC was quenched by AuNPs on the concentration dependent manner, and the equilibrium constants for the sorption of TC on the NP surface were calculated. Significant increase of fluorescence quenching was noticed when NP size increased, keeping the concentration of NPs of different size constant. By comparing experimental and calculated results for quenching of TC dye fluorescence, we assumed that the maximum quenching was restricted to full monolayer coverage of TC on the NP surface. The conclusion was drawn that the most probable orientation of TC dye molecules on the NP surface was slanted and that the dye approached NP surface with its positively charged thiazole ring.



INTRODUCTION

Cyanine dyes belong to an important class of organic compounds which have become of great interest, both from scientific and practical points of view. These compounds have strong absorption in the visible region and are highly fluorescent in monomers and aggregates, both in solution and organized media.^{1–3} The self-association of cyanine dyes results in the formation of associates, such as dimers and H- and J-aggregates,^{4,5} which are composed of many thousands of dye monomers.

Numerous studies were carried out with cyanine dyes of different structures in solutions, in the presence of protein molecules, surfactants, polymers, metal ions, and NPs. Adsorption of molecules on the surfaces for studying photophysical and photochemical processes contributed to the elucidation of adsorption kinetics and evaluation of effects of chain length of alkyl group.⁶ Several studies focused on the study of self-assembly of cyanine dyes on the surface of charged polymers, and the kinetic aspects of aggregation processes were discussed.^{7,8}

There is a growing interest in the study of NPs mediated self-organization of these molecules due to their new application for chemical sensing,^{9–11} catalysis,^{12,13} drug delivery,¹⁴ nanoelectronics,¹⁵ and medical diagnostics.^{16,17} The dye molecules are adsorbed in a flat geometry in the monomer form,¹⁸ with a maximum interaction between the dye and the metal NP surface. Considering the general structure of thiacyanine dyes,

the adsorption occurs due to the Coulombic interactions between nitrogen or sulfur atoms with the NP surface.¹⁹ The strength of these interactions depends on spatial and spectral overlap between the plasmonic structure and molecular aggregates and determines both the absorption and emission properties of molecules coupled to NPs.^{20–22} The experimental and theoretical results revealed that optical properties of composite NPs consisting of a metal core (Au, Ag, Cu, and Al) and some cyanine dyes (TC, OC, and PIC) can be markedly improved by coating NPs with a thin layer of dye molecules in a J-aggregate state.^{23–25} Several papers reported the synthesis of core–shell systems with the optical properties dependent on NPs size, shape, and spacer layer^{26,27} which promoted the J-aggregation of anionic cyanine dyes on the NPs surface. The absorption spectra of these systems are characterized by a distinct peak or deep near J-band, which indicates the way of plasmon–exciton interaction.^{27–29} Furthermore, there are various examples in the literature in which the adsorption of fluorescein dye on the metal NPs do not induce forming molecularly organized J- or H-aggregates.^{30,31} However, some studies on AuNPs–organic molecules composites revealed that smaller particles stimulated J-aggregation on the metal particle surface, whereas larger particles did not induce any kind of

Received: November 7, 2012

Revised: March 11, 2013

Published: March 12, 2013



aggregation.^{32–34} Our findings suggest that both the size of NPs as well as their surface conditions resulting from the reducing agents might play a crucial role whether the formation of J-aggregate or just adsorption of the dye was occurred.^{35,36}

Since cyanine dyes are highly fluorescent,¹ the measurements of fluorescence properties of the particle–dye assemblies can provide important insight into the understanding of the interparticle molecular interactions and reactivity. Fluorescent labeling is widely used for biological imaging in medical diagnostics³⁷ to simulate drug release or to localize NPs. Recent studies on the photophysical properties of chromophore modified NPs by our group^{35,36} and others^{34,38,39} have suggested an efficient quenching of the fluorescence of the chromophores when they are densely packed on the NPs surface. This quenching is generally ascribed to an increased nonradiative relaxation of the excited state due to the energy and/or electron transfer.^{39,40} On the other hand, a pronounced fluorescence enhancement of chromophores close to the metal surface has been reported.^{41–44} It was found that whether the fluorescence quenching or enhancement will occur depends on the competition of two processes, i.e., nonradiative energy transfer from the chromophores to the metal surface and the local field enhancement.⁴⁵ In many of the examples studied to date, the energy transfer from the excited chromophores to the metal surface, which is dependent on the NP size, shape, and the distance between the chromophores and NP surface, is considered to be one of the deactivation pathways in these systems.^{46–51} When chromophores are located in close proximity to the metal surface, nonradiative energy transfer and fluorescence quenching take place. However, local field enhancement and increased radiative rates still occur at longer distances from the metal surface. Furthermore, an inherent problem in the study of fluorescence quenching occurs when another molecule or part of a macromolecule absorbs at the wavelengths at which the fluorophore emits radiation. It is termed the inner filter effect (IFE).⁵² This effect, explained by the emission reabsorption in the sample, whereby some or all of the photons emitted by the fluorophore may be absorbed again, can also occur because of high concentrations of absorbing molecules, including the fluorophore. The result is that the intensity of the excitation light is not constant throughout the solution and only a small percentage of it reaches the fluorophores that are visible for the detection system. It changes the spectrum and intensity of the emitted light, since it depends on the optical density of the sample at both excitation and emission wavelengths and is not the linear function of the chromophore concentration. Several instrumental and mathematical procedures have been proposed to correct for IFE.^{53–55} In some studies of fluorescence quenching of fluorescently labeled AuNPs,^{40,56} the simple correction factor proposed by Lakowitz⁵⁷ was applied to account for IFE.

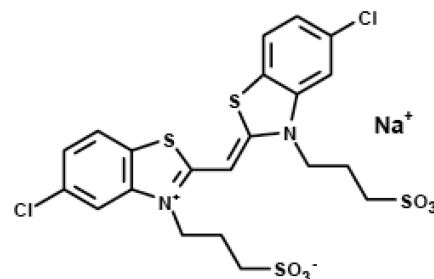
The present paper represents the continuation of our study of interactions between AuNPs and 5,5'-disulfopropyl-3,3'-dichlorothiacyanine dye (TC).^{35,36} The aim of this work was to investigate the adsorption and the fluorescence quenching upon the adsorption of this dye on citrate capped AuNPs with the average core sizes of 9, 17, and 30 nm, denoted as C9, C17, and C30. The characterization of these NPs in the presence and absence of TC dye was performed by using different experimental techniques. The influence of particle size on quenching of the dyes' fluorescence in the presence of the same number of NPs in all three colloidal dispersions has been discussed. By comparison between the experimental results of

fluorescence quenching with those obtained by theoretical calculations, we also predicted the most probable orientation of TC molecules on the NP surface. Since the fluorescence quenching was shown to be quantitatively related to the surface coverage of the dye molecules on the AuNP surface, the sorption parameters were evaluated. Moreover, a series of AuNPs of the same chemical composition, but with different particle sizes, offers the possibility of studying the size-dependent phenomena related to the fraction of dye molecules on the NP surface and also the effects which show behavior due to completion of shell in this system with delocalized electrons.

■ EXPERIMENTAL SECTION

Chemicals. Gold(III) chloride trihydrate ($\text{HAuCl}_4 \cdot 3\text{H}_2\text{O}$), potassium chloride (KCl), and trisodium citrate dihydrate ($\text{C}_6\text{H}_5\text{Na}_3\text{O}_7 \cdot 2\text{H}_2\text{O}$), all from Aldrich, were used as received. Thiacyanine dye (TC; 5,5'-disulfopropyl-3,3'-dichlorothiacyanine sodium salt), the structure illustrated in Scheme 1, was

Scheme 1. TC Dye Structure



purchased from Hayashibara Biochemical Laboratories, Okayama, Japan. Water purified with a Millipore Milli-Q water system was used for preparing all solutions. A 50 μM aqueous TC stock solution, containing 1 mM KCl, was prepared by dissolving the solid TC. The dye working solutions were prepared by appropriate dilution of 50 μM TC stock solution, immediately before measurements.

Synthesis of AuNPs. AuNPs (colloidal dispersions C9, C17, and C30) were prepared using sodium citrate as a reducing agent. According to modified procedure reported by Grabar et al.,⁵⁸ a 200-mL sample of 1 mM HAuCl_4 was brought to a vigorous boiling, in a round-bottom flask fitted with a reflux condenser, with continuous stirring. Then, 45, 20, or 10 mL of 38.8 mM sodium citrate was rapidly added to the boiling solution to prepare colloids C9, C17, and C30, respectively. The solution was boiled for another 15 min, during which time the solution changed color from pale yellow to deep red (wine-red) and then was allowed to cool to room temperature with continued stirring. The size of the nanospheres can be controlled by varying the citrate/gold ratio. Generally, a smaller amount of citrate will yield larger nanospheres.

The concentration of stock dispersion of AuNPs C9, C17, and C30 was determined from the absorbance at the maximum (520, 523, and 527 nm, respectively) and molar extinction coefficient for the corresponding average size of AuNPs (ϵ_λ for C9 from ref 59, ϵ_λ for C17 from ref 60, and ϵ_λ for C30 from ref 61).

Instrumentation. Transmission electron microscopy (TEM) measurements were performed on Hitachi H-7000 and JEOL 100CX microscope instrument at an operating voltage of 100 kV. For each sample, the size of more than 200

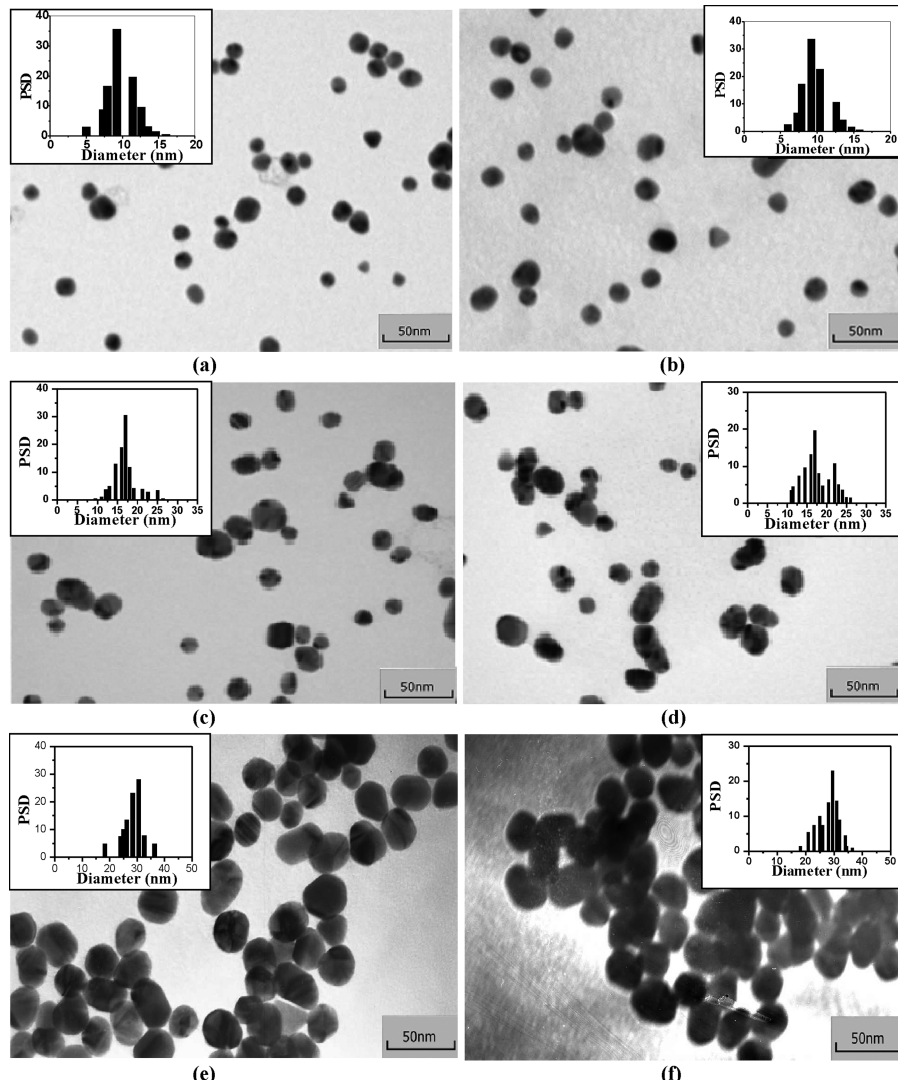


Figure 1. TEM analysis of AuNPs C9, C17, and C30 without (a, c, and e) and with TC dye (b, d, and f) with corresponding particle size distributions (PSD).

particles in the TEM images was measured to obtain the average particles size.

The surface topography of nanoparticles was characterized and analyzed by atomic force microscopy (AFM) on universal scanning probe microscope (USPM), Quesant Instrument Co. The experiments were performed using AFM tips with a tip radius less than 10 nm and with a standard silicon tapping probe with 40 N/m force constant on 350 kHz resolution frequency by Nanoandmore. Samples were prepared by applying a drop of the sample solution onto freshly cleaved mica discs and allowing it to air-dry before measurement. To gather a variety of roughness-related measurements, AFM images were analyzed by using Gwyddion 2.30 data analysis Software.

Dynamic light scattering (DLS) was performed using a Zetasizer Nano, ZS with 633 nm He–Ne laser, equipped with a MPT-2 Autotitrator, Malvern, U.K.. The experimental data were the average of at least eight runs. Each curve/run presents an average result of 14 measurements. The latter instrument can measure particle sizes from 0.6 nm to 6 μm and was also used to determine zeta potentials of the AuNPs and the particle-dye assemblies.

A Perkin-Elmer Lambda 35 UV–vis spectrophotometer was used for measuring the absorption spectra in a quartz cuvette with path length 1 cm.

FTIR spectra of colloidal solutions with and without TC dye were recorded on Thermo Electron Corporation Nicolet 380 FTIR spectrophotometer with an ATR (attenuated total reflection) accessory, equipped with a diamond tip. The spectra were collected over the range of 500–4000 cm^{-1} .

Photoluminescence emission was measured using Fluorolog-3 model FL3-221 spectrofluorometer (HORIBA Jobin-Yvon). Excitation and emission monochromators were double grating, with dispersion of 2.1 nm/mm (1200 grooves/mm), blazed at 406 nm for excitation and 420–600 nm for emission. A xenon lamp provided excitation and fast TBX detector was used for emission measurements in a right angle configuration with a 1 cm path cuvette.

RESULTS AND DISCUSSION

Characterization of AuNPs in the Presence of TC Dye. Three Au colloidal dispersions (C9, C17, and C30) with different NP sizes were prepared and their individual interactions with TC dye were compared. For the study of

Table 1. Average Values of AuNP Diameters (d_{av}) in the Absence and Presence of 1.6×10^{-5} M TC Obtained by TEM and DLS Measurements

d_{av} (nm)	C9		C17		C30	
	without TC	with TC	without TC	with TC	without TC	with TC
TEM	9 ± 1.5	9 ± 2.4	17 ± 2.7	17 ± 3.2	30 ± 3.7	30 ± 3.9
DLS	11 ± 1.8	11 ± 2.3	19 ± 2.4	19 ± 2.8	33 ± 2.9	33 ± 3.6

Table 2. Zeta Potential and Conductivity for Au Colloids in the Absence and Presence of 1.6×10^{-5} M TC Dye

colloid	NP conc. (M)	pH	zeta potential (mV)		conductivity ($\mu\text{S}/\text{cm}$)	
			without TC	with TC	without TC	with TC
C9	4.2×10^{-8}	6.5	-48.3 ± 1.4	-44.1 ± 0.9	1200 ± 16	983 ± 9
C17	0.74×10^{-8}	5.59	-43.9 ± 1.3	-41.8 ± 0.9	1060 ± 14	768 ± 9
C30	0.18×10^{-8}	3.81	-38.0 ± 0.8	-35.8 ± 0.9	649 ± 2	498 ± 4

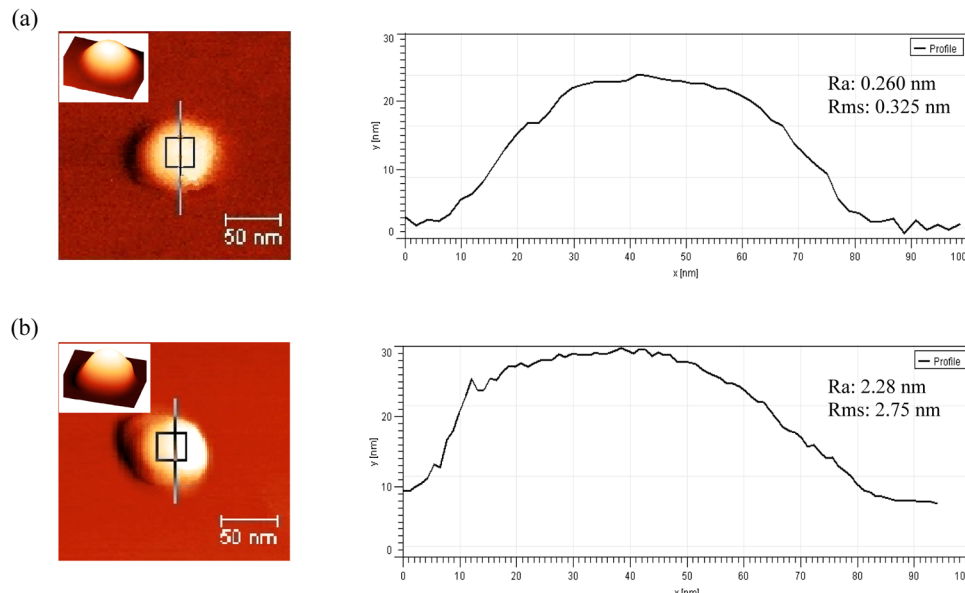


Figure 2. Topographical AFM images of the surface of AuNP C30 without (a) and with (b) TC dye with the corresponding AFM cross section analysis. The insets show nanoparticles in 3D topography.

the interference of NPs with TC dye, colloidal dispersions were mixed with TC, and the final concentration of TC was 1.6×10^{-5} M. The shape and size distribution of the AuNPs were examined by TEM. Typical TEM images of colloidal dispersions before and after the addition of TC dye are presented in Figure 1.

On the basis of TEM measurements, the net AuNPs (Figure 1a, c, and e) are nearly spherical in shape with a relatively narrow size distribution (Table 1).

It should also be noted that the adsorption of TC dye on the AuNPs has no influence on the particles size and agglomeration (Figure 1b, d, and f), implying the effective stabilization by citrate ions.

The particle size distribution measurements by DLS method were also performed, using NP dispersions before and after the addition of TC dye. The obtained average particle diameter represents the hydrodynamic diameter of a sphere (i.e., diameter of particle with hydration shell), having the same volume as the particle (Table 1). The comparison of results obtained by TEM and DLS measurements indicated that particle sizes obtained by TEM were smaller than that obtained by DLS, since the particle size obtained by DLS measurements

included the added solvent or stabilizer moving with the particle.

Zeta potential and conductivity for initial Au colloidal dispersions were measured in the absence and presence of TC dye. As shown in the Table 2, if the amount of the negatively charged capping agent increases, the absolute value of the zeta potential increases. Moreover, the addition of TC dye in colloidal dispersions induced the slight decrease of the zeta potential due to the weak electrostatic interactions between the trivalent citrate anions and the positively charged thiazole moiety of the TC dye. The result of this interaction is the partial neutralization of the zeta potential of AuNPs. The addition of TC dye in colloidal dispersions did not change the pH values.

The results presented in Table 2 also indicated conductivity decrease when the TC dye was added to colloidal dispersions C9, C17, and C30, which is in accordance with the results obtained by the zeta potential measurements.

Surface morphology before (Figure 2a) and after the dye adsorption on the AuNP C30 surface (Figure 2b) was analyzed using AFM. Surface irregularities were displayed in a profile graph obtained by drawing a 100 nm cross-sectional line across the particle, and an image segment within the particle (marked

as square in Figure 2) was used for calculating Ra (the arithmetic average of the roughness profile) and Rms (root-mean-square roughness) values, indicative for expressing surface roughness using statistical roughness analysis function. The results obtained from section analysis indicated that the roughness of a NP or selected region inside the particle increased upon the dye adsorption (Ra and Rms value for the selected surface area increased), which may be considered as indirect evidence of dye molecules residing on the surface of NPs. A specialized computer program (Gwyddion 2.30) was used to perform the statistical analysis and to obtain nanoparticles in 3D topography (insets in Figure 2). 3D topography gave additional insight into the characteristics of the nanoparticle surface.

The absorption spectrum of the dye in aqueous solution (Figure 3, line 1), shows a short-wavelength maximum at 409

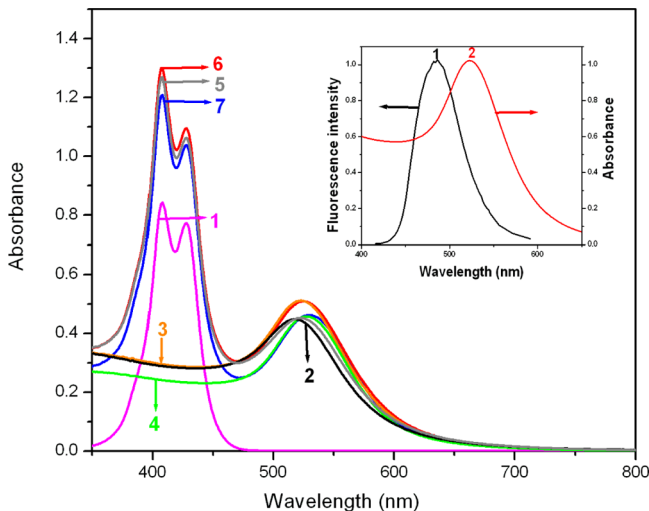


Figure 3. Absorption spectra of (1) TC dye (1.6×10^{-5} M), (2) colloid C9 (1.9×10^{-9} M), (3) colloid C17 (8.7×10^{-10} M), and (4) colloid C30 (2×10^{-10} M) and solutions containing 1.6×10^{-5} M TC upon the addition AuNPs: (5) colloid C9 (1.9×10^{-9} M), (6) colloid C17 (8.7×10^{-10} M), and (7) colloid C30 (2×10^{-10} M). Inset: normalized fluorescence spectrum of TC (1) and absorption spectrum of C17 (2).

nm denoted as D-band which is assigned to the dimer (TC_2^{2-}) and a long-wavelength maximum (M-band) at 429 nm assigned to the monomer (TC^-).³³

The dye is present as an equilibrated mixture of monomers and dimers.⁶² On the other hand, AuNPs C9, C17, and C30 have a surface plasmon resonance (SPR) band with the maximum between 520 and 530 nm (Figure 3, lines 2–4). Table 3 lists the spectral characteristics in the presence and absence of TC dye. The molar extinction coefficients given in Table 3 were used to calculate the initial concentrations of NPs in colloidal dispersions given in Table 2. However, since for the

Table 3. Spectral Characterization of Colloidal Dispersions in the Presence and Absence of 1.6×10^{-5} M TC Dye

colloid	λ_{max} [nm]		ϵ_{λ} [$\text{M}^{-1} \text{cm}^{-1}$]
	without TC	with TC	
C9	520	523	2.4×10^8
C17	523	526	6×10^8
C30	527	530	3×10^9

particles of the selected size synthesized in this work the scattering coefficient is negligible,^{63,64} the molar extinction coefficient is equal to the molar absorption coefficient, and the absorption cross section was used throughout this work.

In general, the position of the plasmon band is usually dependent on the synthesis procedure, size, shape, interparticle distances and surrounding dielectric medium constant.^{65–67} Absorption spectra of nanoparticle–dye assemblies, Figure 3 (lines 5–7), did not indicate any observable reactivity, except the red shift (3 nm) of the plasmon band due to the change in the refractive index around the particles in the presence of TC dye. This indicates good stability of these particles which could be explained by the stabilization of the particles by citrate ions adsorbed at the surface of particles, consistently with TEM measurements. Furthermore, the adsorption of TC dye occurs predominantly by weak interaction between the TC and ions adsorbed at the surface of the particles. However, the solutions remained clear with no evidence of particle precipitation.

FTIR Spectra of AuNPs in the Presence of Dye. To understand the interaction between the TC dye and Au colloids, FTIR spectra of the TC dye–Au colloid assembly were measured and compared with those of the neat TC dye and Au colloid. As an example, corresponding spectra in the case of colloid C30 are presented in both high and low frequency regions, Figure 4. Similar results were obtained in the case of colloid C9 and C17 (spectra not shown).

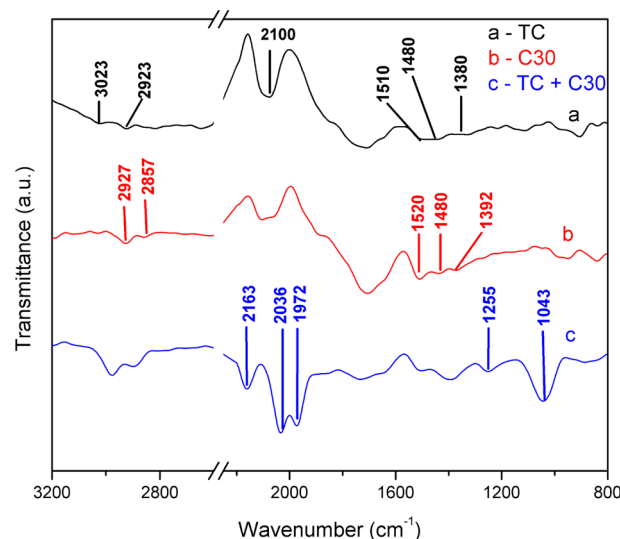


Figure 4. FTIR spectra of (a) TC dye, (b) citrate capped AuNPs (colloid C30), and (c) TC dye–Au colloid C30 assembly.

The characteristic bands in the FTIR spectrum of the TC dye, Figure 4a, appeared around 3023 cm^{-1} (CH stretching vibration associated with the double bonds), 2923 cm^{-1} (aliphatic CH stretching bands), 2100 cm^{-1} (stretching vibrations of $-\text{SCN}$ groups), 1510 cm^{-1} (weak band corresponding to stretching vibrations of $\text{C}=\text{N}$ of the thiazole ring), 1380 and 1480 cm^{-1} (ring stretching modes), and 900 – 780 cm^{-1} (weak set of absorptions associated with banding vibrations in the aromatic structure). In the FTIR spectrum of citrate capped AuNPs, Figure 4b, a weak but distinct set of absorptions was observed at 2927 – 2857 cm^{-1} , assignable to CH stretching vibrations of CH_2 groups of citrate while bands at 1520 and 1480 cm^{-1} correspond to asymmetrical and symmetrical stretching vibrations of carboxylates, respectively.

The bands of TC dye–Au colloid assembly, Figure 4c, were in the same regions and had the same features as those of the neat TC and citrate capped AuNPs, with the following exceptions: (1) the band at 2898 cm^{-1} (due to the stretching vibrations of CH_2 groups) is broadened and clearly shifted relative to that band of the neat citrate capped Au, (2) the band at 2977 cm^{-1} ($\text{C}-\text{H}$ from $\text{Ar}-\text{H}$ stretch) is shifted to lower frequencies relative to that of the neat TC dye, (3) absorption at 2100 cm^{-1} corresponding to stretching vibrations of $-\text{SCN}$ group is shifted to 2163 cm^{-1} and additional twin bands are observed at 2036 and 1972 cm^{-1} , (4) the bands at 1392 cm^{-1} (ring stretching mode) and 1255 cm^{-1} ($\text{C}-\text{O}$) were shifted and increased in intensity, and (5) an additional band observed at 1043 cm^{-1} has been assigned to the frequency combination of ($\text{C}-\text{O} + \text{S}=\text{O}$) vibrations. The increasing intensity of two bands at 1255 and 1043 cm^{-1} indicated the interaction of the $\text{C}-\text{O}$ bond of ester group of trisodium citrate with molecules of TC dye. Water present in measured samples may have resulted in the broad band in the region of 1620 – 1730 cm^{-1} visible in all three spectra. The intensity of this band, relative to that of the neat TC dye, increased in the case of AuNPs, Figure 4b, due to the stretching mode of carboxylic acid ($\gamma(\text{COOH})$). In the TC dye–Au colloid assembly, Figure 4c, this band decreased in intensity and almost disappeared. These findings indicated that the adsorption of TC dye is only possible if the dye molecules are oriented toward the negatively charged surface of NPs via thiazole ring, which carries a partial positive charge. It is important to notice that the thiazole ring is characterized by large π -electron delocalization and that the positive charge of sulfur increases in the presence of positive nitrogen.¹⁹ However, due to the steric consideration, the propylsulfonate group can adopt a stable conformation which brings the nitrogen and sulfur atoms nearer. This effect leads to the increased positive charge on the nitrogen while the sulfur becomes less positive. This allows us to emphasize that the interaction between the dye and AuNPs is not strong and occurs by a combination of π - π and the electrostatic interactions between the positive thiacyanine groups of the dye and the negative citrate on the particle surface. Moreover, the absorption and emission spectra of TC did not change upon the adsorption on AuNPs. Also, there was no change in the absorption spectrum of the AuNPs upon the dye adsorption; that is, there was no damping or broadening of the SPR band. Therefore, we could exclude any type of covalent bonding such as $\text{Au}-\text{S}$ or $\text{Au}-\text{N}$ and confirm that the interaction between the dye and AuNPs occurs through the noncovalent bonding (weak electrostatic interaction). The previous infrared spectroscopic study³⁴ showed that the interaction occurs between the positively charged ammonium moiety of cyanine dye and the negatively charged carboxylate on the AuNP surface. It is important to note that the observation of the weak electrostatic interaction between the dye and AuNPs, in the present work, is in fact consistent with the UV-vis measurements and the fact that this interaction was not followed by particle aggregation or J-aggregation. Also, this kind of interaction often leads to the close packing of dye molecules on the charged NPs surface.³⁶

Fluorescence Quenching of TC Dye by AuNPs. For the study of the influence of AuNPs on the TC fluorescence, two series of experiments were performed by mixing TC dye and colloidal dispersions C9, C17, and C30. In the first set of measurements the final concentration of TC was $1.0 \times 10^{-6}\text{ M}$,

whereas C9, C17, and C30 concentrations varied from 4.76×10^{-11} to $4.44 \times 10^{-9}\text{ M}$.

TC dye exhibits a strong fluorescence with emission maximum at 485 nm (the excitation wavelength λ_{ex} was 406 nm) in aqueous solution (Figure 5, line 1).⁶⁸ Under these

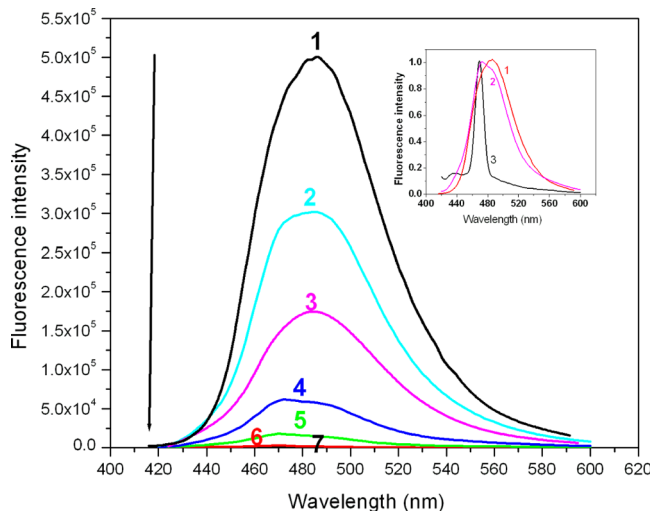


Figure 5. Change of fluorescence spectra of $1 \times 10^{-6}\text{ M}$ TC upon the addition of C17 colloid as the dependence on AuNPs concentration. (1) TC, $1 \times 10^{-6}\text{ M}$; concentration of AuNPs: (2) $4.9 \times 10^{-10}\text{ M}$, (3) $9.85 \times 10^{-10}\text{ M}$, (4) $1.48 \times 10^{-9}\text{ M}$, (5) $2.47 \times 10^{-9}\text{ M}$, (6) $3.45 \times 10^{-9}\text{ M}$, and (7) $4.44 \times 10^{-9}\text{ M}$. Inset: Comparison of normalized fluorescence spectra of TC in the absence (1) and presence of C17 (2) with the water Raman band (3).

experimental conditions AuNPs do not exhibit fluorescence. In all three colloidal systems it can clearly be seen that the fluorescence intensity of the dye decreased with increasing NP concentration, indicating that the TC dye–Au colloid assembly displayed fluorescence quenching properties. There are various examples in the literature in which the excited-state quenching has been attributed to energy transfer to the metal surface.^{21,34,40,56,69–72} However, in the case of hybrid assemblies with metal NPs as core, the energy transfer depends on the size and shape of the NPs, the distance between the dye and the NPs surface, the orientation of the dye molecular dipole with respect to the dye-NP axis, and the overlap of the dye emission with the NPs absorption.⁴⁰ In the present case, as indicated in Figure 3 (inset), fluorescence spectra of TC dye overlap with the absorptions of the AuNPs, allowing us to expect the energy transfer from the excited TC molecule to the AuNP surface. It was observed earlier that the surface plasmon acts as an efficient energy acceptor even at a distance of 1 nm between dye molecules and gold surfaces.⁷³ It is important to know that, in the investigated systems (C9, C17, and C30), the citrate layer on the AuNPs is thin enough ($<0.6\text{ nm}$)⁷⁴ to allow near-field interaction between the dye and AuNP surface. Furthermore, the fluorescence quenching is tested on small TC molecules,³⁴ which are expected to provide relatively short separation distance from the dye molecule to the AuNP ensuring highly efficient quenching. In general, the emission from the chromophores in the close vicinity of metal surface ($<5\text{ nm}$) is mostly quenched because of the excitation energy transfer or the charge transfer to the plasmon of metal NPs.⁴⁰ Also, due to the NP symmetry, the energy transfer to spherical AuNPs can take place for any orientation of the dye transition dipole

moment in respect to the surface of NPs unlike in dye–dye systems.⁷⁵

However, another important effect which could lead to decrease in fluorescence intensity must be taken into account, i.e., the inner filter effect (IFE), photon reabsorption by the mixture components. To account for IFE, the simple correction factor proposed by Lakowicz⁵⁷ was applied to the measured fluorescent spectra, according to the equation:

$$F_{\text{corr}} = F_{\text{obs}} 10^{(A_{\text{ex}} + A_{\text{em}})/2} \quad (1)$$

where F_{corr} and F_{obs} are the fluorescence intensities for the corrected and observed signals and A_{ex} and A_{em} are the solution absorbancies at the excitation and emission wavelengths, respectively. This simple equation was used since it is valid and applicable in the case of typical fluorophores where scattering is negligible and the extinction is dominated by absorption. Therefore, in our calculations the absorption cross section was used.

The raw fluorescence spectra of 1.0×10^{-6} M TC solution before and upon the addition of colloid C17 are shown in Figure 5 (lines 2–7). Similar results were also obtained for colloid C9 and C30 (data not shown).

The spectra presented in Figure 5 are the result of photon emission (radiative decay) obtained from the free (unbound) dye molecules in the solution, which are the only emitting species. It is important to note here that spectra in Figure 5 contain contribution of water Raman scattering (for 406 nm excitation water Raman scattering is peaking at 470.6 nm) which is visible in the presence of high NP concentrations (samples 4–7). Precisely by increasing C17 concentration in the TC solution, the fluorescence intensity decreases due to the quenching effect of NPs. Thereby, the water Raman scattering contribution is not negligible and affects the spectral shape yielding in the slight blue shift of the fluorescence spectra. To illustrate the contribution of water Raman scattering, normalized sharp water Raman band together with fluorescence spectra of TC in the presence and absence of colloid C17 are presented in Figure 5 (inset).

The dependence of the corrected fluorescence intensity of the TC dye at 485 nm vs NP concentrations is shown in Figure 6.

To obtain the experimental titration end points, the curves were extrapolated by straight lines to zero. The obtained final concentrations of NPs in colloidal dispersions needed to achieve titration end points, i.e. to quench the fluorescence of 1×10^{-6} M TC were about 6.5×10^{-9} M for C9, 3.0×10^{-9} M for C17 and 1.1×10^{-9} M for C30. Moreover, we used these concentrations to calculate the number of TC molecules per one NP and the obtained values were 154 TC molecules/C9, 333 TC molecules/C17, and 909 molecules/C30. By dividing these values with the surface area of NP (see Table 4), we obtained the surface coverage of NP by TC molecules. The obtained values were 6.06×10^{13} TC molecules/cm² in the case of C9, 3.67×10^{13} TC molecules/cm² for C17, and 3.22×10^{13} TC molecules/cm² for C30. In addition, Figure 6 (inset) shows the influence of particle size on quenching of TC dyes' fluorescence in the presence of the same number of NPs in all three colloidal dispersions. The obtained results indicated that the percent of experimentally obtained fluorescence quenching increased with NP diameter. This observation is consistent with the results presented in ref 34. Moreover, although bigger AuNPs possess lower surface energy than the smaller ones, the

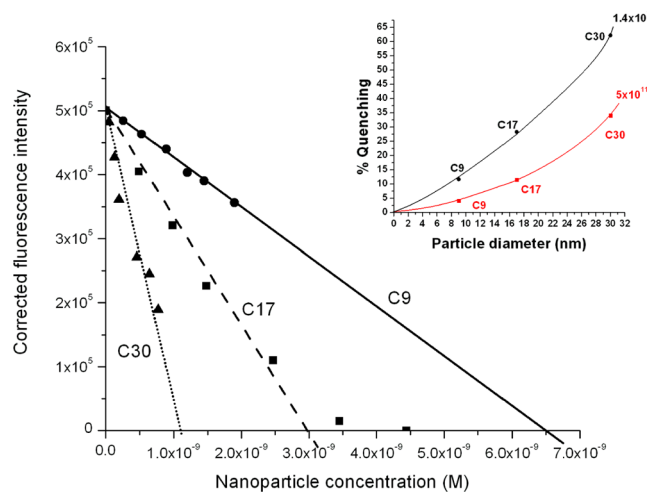


Figure 6. Dependence of corrected fluorescence intensity (at 485 nm) of the solution containing 1×10^{-6} M TC and AuNPs of different sizes vs NP concentrations. Inset: influence of particle size on quenching of TC dyes' fluorescence in the presence of 1.4×10^{12} and 5×10^{11} NPs in 3 mL.

obtained results correlate with the surface area availability of AuNPs, since bigger particles possess higher surface area available for the adsorption of dye. Consequently, a higher amount of dye molecules can be accommodated on their surface and be quenched. It is also important to note that for NP concentrations which are high enough the fluorescence emission is totally quenched; that is, the NPs are able to completely quench the emission upon fluorophore adsorption. Thereby, the quenching efficiency for all investigated NPs is considered constant.

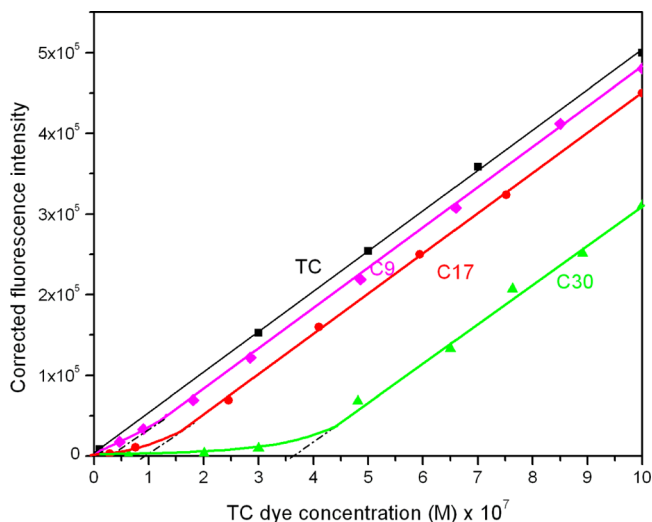
In the second set of experiments the fluorescence intensity of TC dye was measured, keeping the NPs concentration 2.8×10^{-10} M (5×10^{11} NPs in 3 mL) constant. The concentration of TC was varied from 1×10^{-8} to 1×10^{-6} M. The dependence of fluorescence intensity corrected for IFE at 485 nm vs TC concentration is presented in Figure 7.

From the straight lines extrapolated to zero fluorescence intensity (Figure 7) it was obvious that no fluorescence was observed when the concentration of TC was less than 0.3×10^{-7} M for C9, 0.9×10^{-7} M for C17, and 3.6×10^{-7} M in the case of C30, which are the concentrations of the dye when the AuNPs surface is saturated with TC molecules. Moreover, as in the case of constant TC concentration (Figure 6), we used these concentrations to calculate the number of TC molecules per one NP, and the obtained values were 108 TC molecules/C9, 323 TC molecules/C17, and 1288 TC molecules/C30. The coverage of the NP surface with TC dye molecules was also quantified, and the obtained values were 4.25×10^{13} TC molecules/cm² in the case of C9, 3.57×10^{13} TC molecules/cm² for C17, and 4.56×10^{13} TC molecules/cm² for C30. Further addition of TC to the colloidal dispersions led to an increase in the emission intensity due to the fluorescence from the TC dianion in the bulk of the solution, without any indication of dye aggregation. For comparison, the concentration dependent fluorescence of TC is also presented in Figure 7.

Assuming that the quenching occurs only for those TC molecules that have direct interaction with the AuNP surface, the maximum of the quenched TC dye is then restricted to full monolayer coverage of TC on the NPs surface, which depends

Table 4. Calculated Number of TC Molecules Adsorbed on NPs C9, C17, and C30

colloid	SAnp (nm ²)	no. of TC dye molecules needed to cover the NPs surface per 3 different orientations				Γ_0 (mol/cm ²)		
		flat	vertical along the long side	vertical along the short side	average no.	flat	vertical along the long side	vertical along the short side
C9	254	67	195	325	195	4.4×10^{-11}	1.3×10^{-10}	2.1×10^{-10}
C17	907	241	698	1163	701			
C30	2826	753	2173	3623	2183			

Figure 7. Dependence of corrected fluorescence intensity at 485 nm on TC concentration for C9, C17, and C30, in the presence of 5×10^{11} NPs.

on the orientation of the adsorbed TC. Taking into account that the dye can be approximated as a rectangular box with dimensions $2.5 \text{ nm} \times 1.5 \text{ nm} \times 0.52 \text{ nm}$,³⁴ three possible orientations of TC on the NP surface can be considered (the flat orientation and vertical orientation along the long and short side). The number of TC molecules needed to cover the NPs surface was calculated and presented in Table 4, together with the number of TC moles per cm² for three possible dye orientations. Lower limit of coverage would be for a flat orientation of TC adsorbing on the surface, whereas an upper limit value would be for a vertical adsorbing orientation along the short side.

By using the values from Table 4, where SAnp represents the surface area of a sphere NPs, with diameter obtained from TEM measurements, and Γ_0 is the maximum monolayer surface coverage (mol/cm²), we calculated the concentration of NPs which could completely quench 1×10^{-6} M TC in the first set of measurements. The values 8.3×10^{-9} M for C9, 4.1×10^{-9} M for C17, and 1.3×10^{-9} M for C30 were obtained. By this calculation it was assumed that the dye molecules were accommodated on the NPs surface in flat orientation. The experimentally obtained results in the first set of measurements (NPs concentration needed to completely quench TC dye fluorescence) are about 20% lower than the calculated values of NPs concentration needed to achieve the titration end point.

In addition, we calculated the TC concentration needed to cover the NPs surface in flat orientation and be completely quenched, in the second set of experiments. The values 1.9×10^{-8} for C9, 6.6×10^{-8} M for C17, and 2.1×10^{-7} M for C30 were obtained, which are about 35% lower than the same values obtained experimentally (Figure 7).

Furthermore, the percentage (%) of the dye being quenched by AuNPs was calculated assuming that one NP can adsorb the number of dye molecules as presented in Table 4 for flat orientation. The quenching efficiencies of 1×10^{-6} M TC by these colloids were compared between the calculated and experimental data (Figure 6), based on the change of fluorescence intensity upon the addition of different quantities of NPs. The results are presented in Table 5.

In general, the experimentally obtained results indicate that more TC molecules are quenched than needed to cover the NPs surface completely in the flat orientation of TC. For example, in the case of colloid C17, the addition of 1.78×10^{12} AuNPs into the dye solution containing 1.8×10^{15} TC molecules is expected to quench 23.8% of the dye in the theoretical calculation for flat orientation. The experimentally obtained change in fluorescence intensity showed that the

Table 5. Fluorescence Quenching at 485 nm of 1×10^{-6} M TC Dye Solution (1.8×10^{15} Molecules of TC) by AuNPs C9, C17, and C30

C9				C17				C30			
% of TC dye being quenched by C9		% of TC dye being quenched by C17		% of TC dye being quenched by C30							
calculated-flat orientation	experimental	corrected fluorescence intensity (485 nm) $\times 10^5$	no. of Au particles $\times 10^{12}$	calculated-flat orientation	experimental	corrected fluorescence intensity (485 nm) $\times 10^5$	no. of Au particles $\times 10^{12}$	calculated-flat orientation	experimental	corrected fluorescence intensity (485 nm) $\times 10^5$	no. of Au particles $\times 10^{11}$
0	0	5.00	0	0	0	5.00	0	0	0	5.00	0
3.1	3.2	4.84	0.47	11.9	19.0	4.05	0.88	3.6	3.6	4.82	0.86
6.4	7.4	4.63	0.95	23.8	35.8	3.21	1.78	9.8	14.6	4.27	2.35
10.7	12.0	4.40	1.60	35.7	54.8	2.26	2.67	14.7	27.8	3.61	3.52
14.5	19.4	4.03	2.16	59.7	78.0	1.10	4.46	34.9	45.8	2.71	8.35
17.5	22.0	3.90	2.61	83.4	97.0	0.15	6.23	48.9	51.0	2.45	11.70
22.9	28.9	3.56	3.42	>100	>100	0	8.02	58.6	62.2	1.89	14.00

fluorescence of 35.8% TC molecules was quenched. Results from both sets of experiments and their comparison with calculated results allowed us to suppose that TC molecules most probably accommodate nearly flat on the metal surface, which is in the slanted orientation. This result is in accordance with the previous studies, which have shown that the fluorescence rate of the dye molecules is a function of the distance between the dye and the metal surface, and that in direct contact with the metal the fluorescence of dye is completely quenched.^{34,38,39} Moreover, our FTIR results confirm that the interaction of TC dye with NPs occurs due to the electrostatic and $\pi - \pi$ interactions between the positive thiacyanine groups of the dye and negative citrate on the NPs surface, which is in accordance with slanted orientation of TC molecules.

However, the NPs surface roughness which could be significant at the scale of dye molecule, thus leading to an increase in effective surface (and consequently to the increased number of quenched TC dye molecules in theoretical calculations), was not taken into account.

In order to further elucidate the influence of NPs on the dye fluorescence, the dependence of corrected fluorescence intensity vs concentration of nanoparticles in solution, presented in Figure 6 was analyzed. On the basis of the above presented experimental results, the adsorption of TC on the surface of the NPs can be described by eq 2, similarly as shown by Zhong and co-workers:³⁴



The equilibrium of eq 2 can be described by a Langmuir type isotherme:

$$K = \frac{\theta_1}{(1 - \theta_1)C_1} \quad (3)$$

where K represents equilibrium constant, C_1 the concentration of TC dye in the solution, and θ_1 the surface fractional coverage of TC on the negatively charged AuNPs. As shown earlier,³⁴ $\theta_1 = \Gamma_1/\Gamma_0$, where Γ_1 represents the surface coverage (moles per cm^2) of TC and Γ_0 the maximum monolayer surface coverage (Table 4). C_0 represents the initial concentration of TC ($C_1 = C_0 - C_{\text{ads}}$).

It can easily be shown that the intensity of the fluorescence of the free dye in the solution is a linear function of the concentration of NPs and that the following equation can be developed, as shown earlier:³⁴

$$I = (-k'bN_0\Gamma_0SA_{\text{NP}})C_{\text{NP}} + k'b\left(C_0 - \frac{1}{K}\right) \quad (4)$$

where $I = k'bC_1$, b is the cell path length, k' is the constant proportional to the quantum yield, the power of incident light and the molar absorptivity of the dye.^{57,76} The values of equilibrium constants K (eq 3) for these colloids were obtained from the slope and the intercept of eq 4 and are given in Table 6.

Table 6. Equilibrium Constants for Process of TC Sorption on the AuNPs

colloid	intercept $\times 10^5$	slope $\times 10^{14}$	$K [\text{M}^{-1}]$
C9	5 ± 0.05	-0.77 ± 0.05	1.79×10^6
C17	5 ± 0.05	-1.67 ± 0.05	3.67×10^6
C30	5 ± 0.05	-4.54 ± 0.1	5.93×10^6

It can be seen that the similar values of K for both colloidal dispersions were obtained, which are comparable by the value obtained by Lim et al.³⁴ for the sorption of similar cyanine dyes on citrate capped AuNPs.

CONCLUSION

The characterization of citrate capped AuNPs with diameter sizes of 9, 17, and 30 nm in the presence and absence of 5,5'-disulfopropyl-3,3'-dichlorothiacyanine (TC) was performed by using TEM, AFM, DLS, zeta potential, FTIR, spectrophotometry, and fluorescence spectra measurements. It was concluded that the adsorption of TC dye on the NPs surface, whereby the particle diameter only insignificantly increased, involved weak electrostatic interactions between the negatively charged carboxylates on the AuNPs surface and the positively charged thiazole moiety of the TC dye. A result of this interaction is the partial neutralization of the zeta potential of AuNPs with TC molecules on their surfaces.

The measurements of fluorescence corrected for IFE of the particle-dye assembly in the presence of constant concentration of TC or NPs clearly indicated the fluorescence quenching properties of AuNPs. Titration end points were determined in all colloidal dispersions for two sets of experiments, first as the concentrations of TC in the case of constant NPs concentration and second as the amount of NPs in the case of constant TC concentration, needed for complete quenching of TC dyes' fluorescence. Significant increase of fluorescence quenching was noticed when NP sizes increased, keeping the concentration of NPs of different size constant. Based on the comparison of experimentally obtained values for fluorescence quenching with the calculated ones, assuming that TC can be approximated as the rectangular box, the conclusion was drawn that the most probable orientation of TC dye molecules on the NPs surface is slanted. This is also supported considering repulsive interactions between the terminal sulfonate groups on the dye and the negatively charged surface of NPs, allowing the dye to approach with its positively charged thiazole ring and to accommodate larger number of TC molecules on the NPs surface. The calculated equilibrium constants for the sorption of TC on the NP surfaces were the same order of magnitude as the values obtained for the sorption of similar cyanine dyes on citrate capped AuNPs.

This work clarifies the interaction of AuNPs with the organic dye and the nature of fluorescence quenching of the dye obtained in their presence. Moreover, AuNPs with different capping agents and with a wider range of diameters will be synthesized, for future use in medical diagnostics, catalysis, drug delivery, nanoelectronics and for chemical sensing. Also, the dependence of the fluorescence excitation and emission of dye-coated particles upon the particle size, the optical properties of the core (silver, gold, etc.), and other terms will be studied further.

AUTHOR INFORMATION

Corresponding Author

*Phone: +381118066428. Fax: +381113408607. E-mail: vodves@vinca.rs.

Notes

The authors declare no competing financial interest.

ACKNOWLEDGMENTS

Authors would thank the Ministry of Education and Science of the Republic of Serbia (Project No. 172023) for their financial support. We are also grateful to Dr. Jasmina Hranisavljević and Dr. Gary P. Wiederrecht for providing us with TC dye and for useful discussion.

REFERENCES

- (1) Benson, R. C.; Kues, H. A. Absorption and Fluorescence Properties of Cyanine Dyes. *J. Chem. Eng. Data* **1977**, *22*, 379–383.
- (2) Slavnova, T. D.; Chibisov, A. K.; Görner, H. Kinetics of Salt-Induced J-aggregation of Cyanine Dyes. *J. Phys. Chem. A* **2005**, *109*, 4758–4765.
- (3) Chibisov, A. K.; Slavnova, T. D.; Görner, H. Self-Assembly of Polymethine Dye Molecules in Solutions: Kinetic Aspects of Aggregation. *Nanotechnol. Russ.* **2008**, *3*, 19–34.
- (4) Kobayashi, T., Ed.; *J-Aggregates*; World Scientific Publishing: Singapore, 1996.
- (5) Hannah, K. C.; Armitage, B. A. DNA-Templated Assembly of Helical Cyanine Dye Aggregates: A Supramolecular Chain Polymerization. *Acc. Chem. Res.* **2004**, *37*, 845–853.
- (6) Behera, G. B.; Behera, P. K.; Mishra, B. K. Cyanine Dyes: Self Aggregation and Behaviour in Surfactants. *J. Surf. Sci. Technol.* **2007**, *23*, 1–31.
- (7) Kaga, K.; Okamoto, K.; Echizen, T.; Karthaus, O.; Nakajima, K. Hierarchic Structure of Cyanine Dyes J-Aggregate in Polymer Microdomes. *Jpn. J. Polym. Sci. Technol.* **2003**, *60*, 752–761.
- (8) Tillmann, W.; Samha, H. J-Aggregates of Cyanine Dyes in Aqueous Solution of Polymers: A Quantitative Study. *Am. J. Undergrad. Res.* **2004**, *3*, 1–6.
- (9) Zheng, W. X.; Maye, M. M.; Leibowitz, F. L.; Zhong, C. J. Imparting Biomimetic Ion-Gating Recognition Properties to Electrodes with a Hydrogen-Bonding Structured Core-Shell Nanoparticle Network. *Anal. Chem.* **2000**, *72*, 2190–2199.
- (10) Han, L.; Daniel, D. R.; Maye, M. M.; Zhong, C. J. Core-Shell Nanostructured Nanoparticle Films as Chemically Sensitive Interfaces. *Anal. Chem.* **2001**, *73*, 4441–4449.
- (11) Zamborini, F. P.; Leopold, M. C.; Hicks, J. F.; Kulesza, P. J.; Malik, M. A.; Murray, R. W. Electron Hopping Conductivity and Vapor Sensing Properties of Flexible Network Polymer Films of Metal Nanoparticles. *J. Am. Chem. Soc.* **2002**, *124*, 8958–8964.
- (12) Narayanan, R.; El-Sayed, M. A. Changing Catalytic Activity During Colloidal Platinum Nanocatalysis Due to Shape Changes: Electron-Transfer Reaction. *J. Am. Chem. Soc.* **2004**, *126*, 7194–7195.
- (13) Zhong, C. J.; Maye, M. M. Core-Shell Assembled Nanoparticles as Catalysts. *Adv. Mater.* **2001**, *13*, 1507–1511.
- (14) Hong, R.; Han, G.; Fernandez, J. M.; Kim, B. J.; Forbes, N. S.; Rotello, V. M. Glutathione-Mediated Delivery and Release Using Monolayer Protected Nanoparticle Carriers. *J. Am. Chem. Soc.* **2006**, *128*, 1078–1079.
- (15) Hicks, J. F.; Zamborini, F. P.; Osisek, A.; Murray, R. W. The Dynamics of Electron Self-Exchange between Nanoparticles. *J. Am. Chem. Soc.* **2001**, *123*, 7048–7053.
- (16) Zheng, W. X.; Maye, M. M.; Leibowitz, F. L.; Zhong, C. J. An Infrared Reflectance Spectroscopic Study of a pH-Tunable Network of Nanoparticles Linked by Hydrogen Bonding. *Analyst* **1999**, *125*, 17–20.
- (17) Taton, T. A.; Mucic, R. C.; Mirkin, C. A.; Letsinger, R. L. The DNA-Mediated Formation of Supramolecular Mono- and Multi-layered Nanoparticle Structures. *J. Am. Chem. Soc.* **2000**, *122*, 6305–6306.
- (18) James, T. H. *The Theory of the Photographic Process*, 4th ed.; Macmillan Publishing Co: New York, 1977.
- (19) Jeunieau, L.; Alin, V.; Nagy, J. B. Adsorption of Thiacyanine Dyes on Silver Halide Nanoparticles: Study of the Adsorption Site. *Langmuir* **2000**, *16*, 597–606.
- (20) Wurtz, G. A.; Evans, P. R.; Hendren, W.; Atkinson, R.; Dickson, W.; Pollard, R. J.; Zayats, A. V.; Harrison, W.; Bower, C. Molecular Plasmonics with Tunable Exciton-Plasmon Coupling Strength in J-Aggregate Hybridized Au Nanorod Assemblies. *Nano Lett.* **2007**, *7*, 1297–1303.
- (21) Wiederrecht, G. P.; Wurtz, G. A.; Hranisavljević, J. Coherent Coupling of Molecular Excitons to Electronic Polarizations of Noble Metal Nanoparticles. *Nano Lett.* **2004**, *4*, 2121–2125.
- (22) Wiederrecht, G. P.; Wurtz, G. A.; Bouhelier, A. Ultrafast Hybrid Plasmonics. *Chem. Phys. Lett.* **2008**, *461*, 171–179.
- (23) Lebedev, V. S.; Medvedev, A. S.; Vasil'ev, D. N.; Chubich, D. A.; Vitukhnovsky, A. G. Optical Properties of Noble-Metal Nanoparticles Coated with a Dye J-Aggregate Monolayer. *Quantum Electron.* **2010**, *40*, 246–248.
- (24) Lebedev, V. S.; Vitukhnovsky, A. G.; Yoshida, A.; Kometani, N.; Yonezawa, Y. Absorption Properties of the Composite Silver/Dye Nanoparticles in Colloidal Solutions. *Colloids Surf. A: Physicochem. Eng. Asp.* **2008**, *326*, 204–209.
- (25) Lebedev, V. S.; Medvedev, A. S. Plasmon - Exciton Coupling Effects in Light Absorption and Scattering by Metal/J-Aggregate Bilayer Nanoparticles. *Quantum Electron.* **2012**, *42*, 701–713.
- (26) Lekeufack, D. D.; Brioude, A.; Coleman, A. W.; Miele, P.; Bellessa, J.; Zeng, L. D.; Stadelmann, P. Core-Shell Gold J-Aggregate Nanoparticles for Highly Efficient Strong Coupling Applications. *Appl. Phys. Lett.* **2010**, *96*, 253107/1–253107/3.
- (27) Yoshida, A.; Yonezawa, Y.; Kometani, N. Tuning of the Spectroscopic Properties of Composite Nanoparticles by the Insertion of a Spacer Layer: Effect of Exciton-Plasmon Coupling. *Langmuir* **2009**, *25*, 6683–6689.
- (28) Yoshida, A.; Kometani, N. Effect of the Interaction between Molecular Exciton and Localized Surface Plasmon on the Spectroscopic Properties of Silver Nanoparticles Coated with Cyanine Dye J-Aggregates. *J. Phys. Chem. C* **2010**, *114*, 2867–2872.
- (29) Yoshida, A.; Uchida, N.; Kometani, N. Synthesis and Spectroscopic Studies of Composite Gold Nanorods with a Double-Shell Structure Composed of Spacer and Cyanine Dye J-Aggregate Layers. *Langmuir* **2009**, *25*, 11802–11807.
- (30) Makarova, O. V.; Ostafin, A. E.; Miyoshi, H.; Norris, J. R.; Miesel, D. Adsorption and Encapsulation of Fluorescent Probes in Nanoparticles. *J. Phys. Chem. B* **1999**, *103*, 9080–9084.
- (31) Templeton, A. C.; Wuelfing, W. P.; Murray, R. W. Monolayer-Protected Cluster Molecules. *Acc. Chem. Res.* **2000**, *33*, 27–36.
- (32) Hranisavljević, J.; Dimitrijević, N. M.; Wurtz, G. A.; Wiederrecht, G. P. Photoinduced Charge Separation Reactions of J-Aggregates Coated on Silver Nanoparticles. *J. Am. Chem. Soc.* **2002**, *124*, 4536–4537.
- (33) Kometani, N.; Tsubonihi, M.; Fujita, T.; Asami, K.; Yonezawa, Y. Preparation and Optical Absorption Spectra of Dye-Coated Au, Ag, and Au/Ag Colloidal Nanoparticles in Aqueous Solutions and in Alternate Assemblies. *Langmuir* **2001**, *17*, 578–580.
- (34) Lim, I. I. S.; Goroleski, F.; Mott, D.; Kariuki, N.; Ip, W.; Luo, J.; Zhong, C. J. Adsorption of Cyanine Dyes on Gold Nanoparticles and Formation of J-Aggregates in the Nanoparticle Assembly. *J. Phys. Chem. B* **2006**, *110*, 6673–6682.
- (35) Vujačić, A.; Vasić, V.; Dramićanin, M.; Sovilj, S. P.; Bibić, N.; Hranisavljević, J.; Wiederrecht, G. P. Kinetics of J-Aggregate Formation on the Surface of Au Nanoparticle Colloids. *J. Phys. Chem. C* **2012**, *116*, 4655–4661.
- (36) Vujačić, A.; Vodnik, V.; Sovilj, S. P.; Dramićanin, M.; Bibić, N.; Milonjić, S.; Vasić, V. Adsorption and Fluorescence Quenching of 5,5'-disulfonylpropyl-3,3'-dichlorothiacyanine Dye on Gold Nanoparticles. *New J. Chem.* **2013**, *37*, 743–751.
- (37) Challa, R. K. *Nanomaterials for Medical Diagnosis and Therapy*; Wiley-VCH: Weinheim, Germany, 2007.
- (38) Nerambourg, N.; Werts, M. H.; Charlot, M.; Blanchard-Desce, M. Quenching of Molecular Fluorescence on the Surface of Monolayer-Protected Gold Nanoparticles Investigated Using Place Exchange Equilibria. *Langmuir* **2007**, *23*, 5563–5570.
- (39) Dulkeith, E.; Ringler, M.; Klar, T. A.; Feldmann, J.; Munoz Javier, A.; Parak, W. J. Gold Nanoparticles Quench Fluorescence by

- Phase Induced Radiative Rate Suppression. *Nano Lett.* **2005**, *5*, 585–589.
- (40) Dulkeith, E.; Morteani, A. C.; Niedereichholz, T.; Klar, T. A.; Feldmann, J.; Levi, S. A.; van Veggel, F. C.; Reinhoudt, D. N.; Moller, M.; Gittins, D. I. Fluorescence Quenching of Dye Molecules Near Gold Nanoparticles: Radiative and Nonradiative Effects. *Phys. Rev. Lett.* **2002**, *89*, 203002/1–203002/4.
- (41) Xie, F.; Baker, M. S.; Goldys, E. M. Enhanced Fluorescence Detection on Homogeneous Gold Colloid Self-Assembled Monolayer Substrates. *Chem. Mater.* **2008**, *20*, 1788–1797.
- (42) Sokolov, K.; Chumanov, G.; Cotton, T. M. Enhancement of Molecular Fluorescence near the Surface of Colloidal Metal Films. *Anal. Chem.* **1998**, *70*, 3898–3905.
- (43) Zhu, J.; Zhu, K.; Huang, L. Using Gold Colloid Nanoparticles to Modulate the Surface Enhanced Fluorescence of Rhodamine B. *Phys. Lett. A* **2008**, *372*, 3283–3288.
- (44) Zhang, J.; Lakowicz, J. R. Metal-Enhanced Fluorescence of an Organic Fluorophore Using Gold Particles. *Opt. Express* **2007**, *15*, 2598–2606.
- (45) Weitz, D. A.; Garoff, S.; Gersten, J.; Nitzan, A. The Enhancement of Raman Scattering, Resonance Raman Scattering, and Fluorescence from Molecules Adsorbed on a Rough Silver Surface. *J. Chem. Phys.* **1983**, *78*, 5324–5338.
- (46) Imahori, H.; Kashiwagi, Y.; Endo, Y.; Hanada, T.; Nishimura, Y.; Yamazaki, I.; Araki, Y.; Ito, O.; Fukuzumi, S. Structure and Photophysical Properties of Porphyrin-Modified Metal Nanoclusters with Different Chain Lengths. *Langmuir* **2004**, *20*, 73–81.
- (47) Gueroui, Z.; Libchaber, A. Single-Molecule Measurements of Gold-Quenched Quantum Dots. *Phys. Rev. Lett.* **2004**, *93*, 166108/I–166108/IV.
- (48) Kerker, M.; Blatchford, C. G. Elastic Scattering, Absorption, and Surface-Enhanced Raman Scattering by Concentric Spheres Comprised of a Metallic and a Dielectric Region. *Phys. Rev. B* **1982**, *26*, 4052–4063.
- (49) Gersten, J. I.; Nitzan, A. Photophysics and Photochemistry Near Surfaces and Small Particles. *Surf. Sci.* **1985**, *158*, 165–189.
- (50) Lakowicz, J. R. Radiative Decay Engineering: Biophysical and Biomedical Applications. *Anal. Biochem.* **2001**, *298*, 1–24.
- (51) Stuart, D. A.; Haes, A. J.; Yonzon, C. R.; Hicks, E. M.; Van Duyne, R. P. Biological Applications of Localised Surface Plasmonic Phenomena. *IEE Proc. Nanobiotechnol.* **2005**, *152*, 13–32.
- (52) Parker, C. A.; Rees, W. T. Fluorescence Spectrometry. A Review. *Analyst* **1962**, *87*, 83–111.
- (53) Puchalski, M. M.; Morra, M. J.; von Wandruszka, R. Assessment of Inner Filter Effect Corrections in Fluorimetry. *Fresenius J. Anal. Chem.* **1991**, *340*, 341–344.
- (54) Kubista, M.; Sjöback, R.; Eriksson, S.; Albinsson, B. Experimental Correction for the Inner-Filter Effect in Fluorescence Spectra. *Analyst* **1994**, *119*, 417–419.
- (55) Gu, Q.; Kenny, J. E. Improvement of Inner Filter Effect Correction Based on Determination of Effective Geometric Parameters Using a Conventional Fluorimeter. *Anal. Chem.* **2009**, *81*, 420–426.
- (56) Lu, Y.; Dasog, M.; Leontowich, A. F. G.; Scott, R. W. J.; Paige, M. F. Fluorescently Labeled Gold Nanoparticles with Minimal Fluorescence Quenching. *J. Phys. Chem. C* **2010**, *114*, 17446–17454.
- (57) Lakowicz, J. R. *Principles of Fluorescence Spectroscopy*, 2nd. ed.; Kluwer Academic/Plenum Press: New York, 1999.
- (58) Grabar, K. C.; Freeman, R. G.; Hommer, M. B.; Natan, M. J. Preparation and Characterization of Au Colloid Monolayers. *Anal. Chem.* **1995**, *67*, 735–743.
- (59) Kim, J. Y.; Lee, D. H.; Kim, S. J.; Jang, D. J. Preferentially Linear Connection of Gold Nanoparticles in Derivatization with Phosphoroxylic Oligonucleotides. *J. Colloid Interface Sci.* **2008**, *326*, 387–391.
- (60) Neramour, N.; Praho, R.; Werts, M. H. Hydrophilic Monolayer-Protected Gold Nanoparticles and their Functionalisation with Fluorescent Chromophores. *Int. J. Nanotechnol.* **2008**, *5*, 722–740.
- (61) Butron, A. S.; Mirkin, C. A.; Stoeva, S. I.; Lee, J. S. DNA-Functionalized Gold Nanoparticles as Probes in Biomolecule Detection Assays. *Nanoscape* **2007**, *4*, 3–9.
- (62) Chibisov, A. K.; Görner, H.; Slavnova, T. D. Kinetics of Salt-Induced J-Aggregation of an Anionic Thiacarbocyanine Dye in Aqueous Solution. *Chem. Phys. Lett.* **2004**, *390*, 240–245.
- (63) Hodak, J. H.; Henglein, A.; Hartland, G. V. Photophysics of Nanometer Sized Metal Particles: Electron-Phonon Coupling and Coherent Excitation of Breathing Vibrational Modes. *J. Phys. Chem. B* **2000**, *104*, 9954–9965.
- (64) Jain, P. K.; Lee, K. S.; El-Sayed, I. H.; El-Sayed, M. A. Calculated Absorption and Scattering Properties of Gold Nanoparticles of Different Size, Shape, and Composition: Applications in Biological Imaging and Biomedicine. *J. Phys. Chem. B* **2006**, *110*, 7238–7248.
- (65) Maye, M. M.; Lim, I. I. S.; Luo, J.; Rab, Z.; Rabinovich, D.; Liu, T. B.; Zhong, C. J. Mediator-Template Assembly of Nanoparticles. *J. Am. Chem. Soc.* **2005**, *127*, 1519–1529.
- (66) Lim, I. I. S.; Maye, M. M.; Luo, J.; Zhong, C. J. Kinetic and Thermodynamic Assessments of the Mediator-Template Assembly of Nanoparticles. *J. Phys. Chem. B* **2005**, *109*, 2578–2583.
- (67) Link, S.; El-Sayed, M. A. Size and Temperature Dependence of the Plasmon Absorption of Colloidal Gold Nanoparticles. *J. Phys. Chem. B* **1999**, *103*, 4212–4217.
- (68) Dai, Z.; Dähne, L.; Donath, E.; Möhwald, H. Mimicking Photosynthetic Two-Step Energy Transfer in Cyanine Triads Assembled into Capsules. *Langmuir* **2002**, *18*, 4553–4555.
- (69) Manikandan, P.; Ramakrishnan, V. Spectral Investigations on N-(2-methylthiophenyl)-2-hydroxy-1-naphthalimine by Silver Nanoparticles: Quenching. *J. Fluoresc.* **2011**, *21*, 693–699.
- (70) Zhang, A.; Fang, Y.; Shao, H. Studies of Quenching and Enhancement of Fluorescence of Methyl Orange Adsorbed on Silver Colloid. *J. Colloid Interface Sci.* **2006**, *298*, 769–772.
- (71) Whitmore, P. M.; Robota, H. J.; Harris, C. B. Mechanisms for Electronic Energy Transfer Between Molecules and Metal Surfaces: A Comparison of Silver and Nickel. *J. Chem. Phys.* **1982**, *77*, 1560–1569.
- (72) Waldeck, D. H.; Alivisatos, A. P.; Harris, C. B. Nonradiative Damping of Molecular Electronic Excited States by Metal Surfaces. *Surf. Sci.* **1985**, *158*, 103–125.
- (73) Inacker, O.; Kuhn, H. Energy Transfer from Dye to Specific Singlet or Triplet Energy Acceptors in Monolayer Assemblies. *Chem. Phys. Lett.* **1974**, *27*, 317–321.
- (74) Giersig, M.; Mulvaney, P. Preparation of Ordered Colloid Monolayers by Electrophoretic Deposition. *Langmuir* **1993**, *9*, 3408–3413.
- (75) Saini, S.; Bhowmick, S.; Shenoy, V. B.; Bagchi, B. Rate of Excitation Energy Transfer Between Fluorescent Dyes and Nanoparticles. *J. Photochem. Photobiol. A: Chem.* **2007**, *190*, 335–341.
- (76) Skoog, D. A.; Holler, F. J.; Nieman, T. A. *Principles of Instrumental Analysis*, 5th ed.; Saunders College Publishing: Philadelphia, PA, 1998.